# Transition-density-fragment interaction approach for exciton-coupled circular dichroism spectra.

AUTHOR(S):

Fujimoto, Kazuhiro J

CITATION:

Fujimoto, Kazuhiro J. Transition-density-fragment interaction approach for exciton-coupled circular dichroism spectra.. The Journal of chemical physics 2010, 133(12): 124101.

ISSUE DATE:

2010-09-28

URL:

http://hdl.handle.net/2433/131807

THE JOURNAL OF CHEMICAL PHYSICS **133**, 124101 (2010)

# Transition-density-fragment interaction approach for exciton-coupled circular dichroism spectra

Kazuhiro J. Fujimoto[a)]
*Department of Chemistry, Graduate School of Science, Kyoto University, Sakyo-ku, Kyoto 606-8502, Japan*

(Received 5 June 2010; accepted 27 July 2010; published online 22 September 2010)

A transition-density-fragment interaction (TDFI) method for exciton-coupled circular dichroism (ECCD) spectra is proposed. The TDFI method was previously developed for excitation-energy transfer, which led to the successful estimation of the electronic coupling energy between donor and accepter molecules in xanthorhodopsin [K. J. Fujimoto and S. Hayashi, J. Am. Chem. Soc. **131**, 14152 (2009)]. In the present study, the TDFI scheme is extended to the ECCD spectral calculation based on the matrix method and is applied to a dimerized retinal (all-*trans N*-retinylidene-L-alanine Schiff base) chromophore. Compared with the dipole-dipole and transition charge from ESP methods, TDFI has a much improved description of the electronic coupling. In addition, the matrix method combined with TDFI can reduce the computational costs compared with the full quantum-mechanical calculation. These advantages of the present method make it possible to accurately evaluate the CD Cotton effects observed in experiment. © *2010 American Institute of Physics*. [doi:10.1063/1.3480015]

## I. INTRODUCTION

Circular dichroism (CD) is a well-known phenomenon observed in chiral molecules, which is defined as the difference in the absorption of left- and right-circularly polarized light ($\Delta\varepsilon=\varepsilon_L-\varepsilon_R$).[1] Since characteristic spectral curves are seen in individual chiral molecules, the CD measurement is widely used to determine the absolute configuration of a molecule.[1] In the field of molecular biology, the CD spectroscopy is a valuable tool for analyzing the protein secondary structure like $\alpha$-helices and $\beta$-strands because of its sensitivity.[2–5] In addition, a time-resolved CD (TRCD) technique was developed in 1985,[6] which has been applied to a number of photochemical and biophysical events. Taking advantage of nanosecond time resolution,[7] the TRCD measurement is used for characterizing the reaction mechanism in excited state and for monitoring the conformational changes of proteins.[8,9]

Exciton coupling between two or more molecules is known to have a large effect on the CD curve,[1,10] which is often termed as the exciton-coupled CD (ECCD). To clarify the ECCD mechanism, many theoretical studies were performed so far. As a pioneering study, the coupled oscillator method on the basis of the chiral through-space interactions between two or more chromophores was developed by Kuhn[11] and Kirkwood,[12] and afterwards the method was extended to various studies.[13–17] In 1962, Tinoco[18] proposed the first order perturbation method to be applied for large systems like polypeptides and proteins. On the other hand, Bayley, Nielsen, and Schellman derived the matrix method[19] from the coupled oscillator method and the Frenkel exciton model.[20] Because of the easier treatment, nowadays, the matrix method is preferred to the first order perturbation method for the CD calculations.[21–24] As another approach, the exciton chirality method, which is also based on the coupled oscillator method, was developed by Harada and Nakanishi.[25] The exciton chirality method has a simple and intuitional picture, so that it is accepted as one of the most efficient approaches for interpreting the physical origin of ECCD in organic molecules.[10]

In our previous study, the transition-density-fragment interaction (TDFI) method was proposed for accurately calculating electronic coupling, so-called pseudo-Coulombic interaction (PCI), and it was applied to the excitation-energy transfer from salinixanthin (donor) to retinal (accepter) chromophores in xanthorhodopsin.[26] While the conventional dipole-dipole (dd) method[27,28] completely failed in describing the PCI value, TDFI succeeded in quantitatively estimating the experimental PCI value. Taking into account the correspondence of PCI with the off-diagonal element in the Hamiltonian matrix, the TDFI method is expected to be applicable to the matrix method. In this paper, it is therefore attempted to extend the TDFI method to the ECCD spectral calculations on the basis of the matrix method.[19] The accuracy of the TDFI method is first tested using a dimerized model compound, hence the comparisons of TDFI with the other methods are performed. Based on the successful description of the electronic coupling, the matrix method with TDFI is applied to a dimerized all-*trans N*-retinylidene-L-alanine Schiff base chromophore[29] and succeeds in nicely evaluating the CD Cotton effects observed in experiment.[29] In this study, the electronic polarization effect induced by the intermolecular interactions is also discussed for accurately estimating the diagonal element in the Hamiltonian matrix.

[a)]Electronic mail: kaziee@kuchem.kyoto-u.ac.jp.

 

## II. THEORY

### A. Rotational strength

Rotational strength, $R$, is a theoretical parameter for calculating CD, and it can be represented by two forms. One is called the length form, which is expressed as the imaginary part of the dot product of electric and magnetic transition dipole moments,[30]

$$R_{0k}^{L} = \mathrm{Im}(\langle 0|\hat{\boldsymbol{\mu}}|k\rangle \cdot \langle k|\hat{\mathbf{m}}|0\rangle), \tag{1}$$

where $\langle 0|\hat{\boldsymbol{\mu}}|k\rangle$ and $\langle k|\hat{\mathbf{m}}|0\rangle$ denote the electric and magnetic transition dipole moments between ground and $k$th excited states, respectively. The operators, $\hat{\boldsymbol{\mu}}$ and $\hat{\mathbf{m}}$, are represented as

$$\hat{\boldsymbol{\mu}} = \sum_i \sum_a e\mathbf{r}_{ia}, \tag{2}$$

$$\hat{\mathbf{m}} = \sum_i \sum_a \frac{e}{2mc}(\mathbf{r}_{ia} \times \hat{\mathbf{p}}_{ia}), \tag{3}$$

where $e$ is the elementary charge, $\mathbf{r}_{ia}$ is a position vector of the electron $a$ in the molecule $i$ from the origin, $m$ is the electron mass, $c$ is the velocity of light, and $\hat{\mathbf{p}}_{ia}$ is the linear momentum operator (i.e., $-i\hbar\nabla$) of the electron $a$ in the molecule $i$. Another representation is derived with the following relation between the electric transition dipole moment, $\langle a|\hat{\boldsymbol{\mu}}|b\rangle$, and the corresponding velocity transition dipole moment, $\langle a|\nabla|b\rangle$,[31,32]

$$\langle a|\hat{\boldsymbol{\mu}}|b\rangle = -\frac{e\hbar^2}{(E_a - E_b)m}\langle a|\nabla|b\rangle, \tag{4}$$

where $\hbar$ is Planck's constant divided by $2\pi$ and $E_a - E_b$ is the energy difference between $a$ and $b$ states. Substitution of Eq. (4) into Eq. (1) gives the so-called velocity form[33]

$$R_{0k}^{V} = \frac{e\hbar^2}{(E_k - E_0)m}\mathrm{Im}(\langle 0|\nabla|k\rangle \cdot \langle k|\hat{\mathbf{m}}|0\rangle). \tag{5}$$

While the length form expressed as Eq. (1) has origin-dependence, the velocity form as Eq. (5) is always origin-independent.

### B. The matrix method for the ECCD calculations

The matrix method is well established tool for calculating ECCD spectra.[19] In this section, the matrix method is briefly explained. The total Hamiltonian for $N$ molecules is given by

$$\hat{H} = \sum_i^N \hat{H}_i + \sum_i^N \sum_{j>i}^N \hat{V}_{ij}, \tag{6}$$

where $\hat{H}_i$ is the local Hamiltonian for the molecule $i$ and $\hat{V}_{ij}$ is the Coulombic interactions between the different molecules $i$ and $j$. Assuming the exciton model, each basis function is represented by direct products of the electronic states for the individual molecules,

$$|\Phi_{ia}\rangle = |\varphi_{10} \cdots \varphi_{ia} \cdots \varphi_{N0}\rangle, \tag{7}$$

where $\varphi_{ia}$ denotes the electronic state $a$ for the molecule $i$. In Eq. (7), only the molecule $i$ is in excited state $a$ and the all other molecules are in their ground states. Then, the $K$th excited state for the total system is expressed by a linear combination of Eq. (7) as

$$|\Psi_K\rangle = \sum_i^N \sum_a C_{ia}^K |\Phi_{ia}\rangle. \tag{8}$$

Similarly, the ground state is written like

$$|\Psi_0\rangle = |\varphi_{10} \cdots \varphi_{i0} \cdots \varphi_{N0}\rangle. \tag{9}$$

To determine the expansion coefficients $C_{ia}^K$ in Eq. (8), we need to diagonalize the Hamiltonian matrix $\mathbf{H}$,

$$\mathbf{U}^{-1}\mathbf{H}\mathbf{U} = \mathbf{H_d}. \tag{10}$$

From this procedure, the eigenvalues and the eigenvectors $C_{ia}^K$ are obtained from the diagonal elements of $\mathbf{H_d}$ and from the elements of the unitary matrix $\mathbf{U}$, respectively. If the ground state energy is set to be zero, the eigenvalues directly correspond to the excitation energies for the exciton-coupled systems. Combining the unitary matrix $\mathbf{U}$ with the noninteracting electric and magnetic transition dipole moments ($\boldsymbol{\mu}_l$ and $\mathbf{m}_l$), we can obtain the dipole moments for the exciton-coupled system as

$$\boldsymbol{\mu}'_K = \sum_l U_{lK}\boldsymbol{\mu}_l, \tag{11}$$

$$\mathbf{m}'_K = \sum_l U_{lK}\mathbf{m}_l. \tag{12}$$

Similarly, the noninteracting velocity transition dipole moment $\nabla_l$ can be transformed to

$$\nabla'_K = \sum_l U_{lK}\nabla_l. \tag{13}$$

Substitutions of Eqs. (11)–(13) into Eqs. (1) and (5) provide the rotational strength for the exciton-coupled system in the length and velocity forms, respectively.

### C. The transition-density-fragment interaction method

As found in Sec. II B, the matrix method is based on the Hamiltonian matrix $\mathbf{H}$. In this section, the procedure to construct the Hamiltonian matrix is explained. For simplicity, let us consider only two states for the molecules $I$ and $J$.

First, the two basis functions are expressed by direct products of the electronic states for the molecules $I$ and $J$ as

$$|\Phi_1\rangle = |\varphi_I^e \cdot \varphi_J^g\rangle, \tag{14}$$

$$|\Phi_2\rangle = |\varphi_I^g \cdot \varphi_J^e\rangle, \tag{15}$$

where $\varphi_I^g$ and $\varphi_J^g$ are the ground states for the $I$ and $J$ molecules, respectively, and $\varphi_I^e$ and $\varphi_J^e$ are the excited states. Using these basis functions, the $2\times 2$ Hamiltonian matrix can be represented as

$$\mathbf{H} = \begin{pmatrix} \langle \Phi_1|\hat{H}|\Phi_1\rangle & \langle \Phi_1|\hat{H}|\Phi_2\rangle \\ \langle \Phi_2|\hat{H}|\Phi_1\rangle & \langle \Phi_2|\hat{H}|\Phi_2\rangle \end{pmatrix}. \tag{16}$$

Here, the diagonal elements are written as

$$\langle \Phi_1|\hat{H}|\Phi_1\rangle = \langle \varphi_I^e|\hat{H}_I|\varphi_I^e\rangle + \langle \varphi_J^g|\hat{H}_J|\varphi_J^g\rangle + \langle \varphi_I^e\varphi_J^g|\hat{V}_{IJ}|\varphi_I^e\varphi_J^g\rangle, \tag{17}$$

$$\langle \Phi_2|\hat{H}|\Phi_2\rangle = \langle \varphi_J^e|\hat{H}_J|\varphi_J^e\rangle + \langle \varphi_I^g|\hat{H}_I|\varphi_I^g\rangle + \langle \varphi_I^g\varphi_J^e|\hat{V}_{IJ}|\varphi_I^g\varphi_J^e\rangle. \tag{18}$$

In the framework of the matrix method, since the total ground state energy is taken to be zero, i.e., $\langle \varphi_I^g\varphi_J^g|\hat{H}|\varphi_I^g\varphi_J^g\rangle = 0$, Eqs. (17) and (18) can be written as

$$\langle \Phi_1|\hat{H}|\Phi_1\rangle = E_{\mathrm{ex}}^I + \int d\mathbf{r}_1 \int d\mathbf{r}_2 \frac{[\rho_I^e(\mathbf{r}_1) - \rho_I^g(\mathbf{r}_1)]\rho_J^g(\mathbf{r}_2)}{r_{12}} - \int d\mathbf{r}_1 \sum_{A\in J}^{\mathrm{nucl}} \frac{[\rho_I^e(\mathbf{r}_1) - \rho_I^g(\mathbf{r}_1)]Z_A}{r_{1A}}, \tag{19}$$

$$\langle \Phi_2|\hat{H}|\Phi_2\rangle = E_{\mathrm{ex}}^J + \int d\mathbf{r}_1 \int d\mathbf{r}_2 \frac{[\rho_J^e(\mathbf{r}_1) - \rho_J^g(\mathbf{r}_1)]\rho_I^g(\mathbf{r}_2)}{r_{12}} - \int d\mathbf{r}_1 \sum_{A\in I}^{\mathrm{nucl}} \frac{[\rho_J^e(\mathbf{r}_1) - \rho_J^g(\mathbf{r}_1)]Z_A}{r_{1A}}, \tag{20}$$

$$\rho_X^k(\mathbf{r}) \equiv N_e \int d\mathbf{r}_2 \int d\mathbf{r}_3 \cdots \int d\mathbf{r}_{N_e} \varphi_X^{k^*}(\mathbf{r},\mathbf{r}_2,\mathbf{r}_3,\ldots,\mathbf{r}_{N_e}) \times \varphi_X^k(\mathbf{r},\mathbf{r}_2,\mathbf{r}_3,\ldots,\mathbf{r}_{N_e}), \tag{21}$$

where $\rho_X^k(\mathbf{r})$ is a one-electron density of the molecule $X$ ($X=I$ or $J$) in the state $k$ ($k$=ground or excited states), $E_{\mathrm{ex}}^X$ is the excitation-energy of the noninteracting molecule $X$, $r_{12}$ (or $r_{1A}$) is a distance between the electrons 1 and 2 (or the electron 1 and the nucleus $A$), and $Z_A$ is the charge of the nucleus $A$. In common cases, the diagonal elements are approximated to be $\langle \Phi_1|\hat{H}|\Phi_1\rangle \approx E_{\mathrm{ex}}^I$ and $\langle \Phi_2|\hat{H}|\Phi_2\rangle \approx E_{\mathrm{ex}}^J$ because the rest terms are considered as negligible contributions.[10]

In the matrix method, the off-diagonal elements play significant roles in the degree of exciton coupling, and thus the treatment should be performed with care. To compute the off-diagonal elements, the dd approximation, which is derived from the leading term of the multipole expansion of the electronic coupling, is frequently used because of its simplicity,[27,28]

$$\langle \Phi_1|\hat{H}|\Phi_2\rangle \approx \frac{\boldsymbol{\mu}_I\cdot\boldsymbol{\mu}_J - 3(\boldsymbol{\mu}_I\cdot\mathbf{e}_R)(\boldsymbol{\mu}_J\cdot\mathbf{e}_R)}{R_{IJ}^3} \equiv V_{\mathrm{Coul}}^{\mathrm{dd}}, \tag{22}$$

where $\boldsymbol{\mu}_X$ denotes the electric transition dipole moment of the molecule $X$ ($X=I$ or $J$), and $R_{IJ}$ and $\mathbf{e}_R$ are a distance between centers of the $I$ and $J$ molecules and its unit vector, respectively. To accurately calculate the off-diagonal elements, however, the dd approximation is limited for two molecules that are separated largely compared with their molecular sizes.[27,28] In addition, the dd method has a practical difficulty in the definition of the molecular centers at which the electric transition dipole moments are placed.

The TDFI method[26] was developed for calculating PCI. In our previous study, TDFI was applied to the excitation-energy transfer in xanthorhodopsin, which resulted in the successful description on the PCI value between the salinixanthin and retinal chromophores. Because the expression of PCI is equal to that of the off-diagonal element in Eq. (16), TDFI is applicable to the matrix method. Taking into account the orthogonality of the electronic states for the $I$ and $J$ molecules, contributions of one-electron integrals and those of two-electron integrals within each of the $I$ and $J$ molecules vanish, and the off-diagonal elements are then given only by the intermolecular electronic Coulombic term, $V_{\mathrm{Coul}}$, as expressed by

$$\langle \Phi_1|\hat{H}|\Phi_2\rangle = \langle \Phi_1|\hat{V}_{IJ}|\Phi_2\rangle = \int d\mathbf{r}_1 \int d\mathbf{r}_2 \frac{\rho_J^{eg}(\mathbf{r}_1)\rho_I^{eg}(\mathbf{r}_2)}{r_{12}} \equiv V_{\mathrm{Coul}}, \tag{23}$$

$$\rho_X^{eg}(\mathbf{r}) \equiv N_e \int d\mathbf{r}_2 \int d\mathbf{r}_3 \cdots \int d\mathbf{r}_{N_e} \varphi_X^{g^*}(\mathbf{r},\mathbf{r}_2,\mathbf{r}_3,\ldots,\mathbf{r}_{N_e}) \times \varphi_X^e(\mathbf{r},\mathbf{r}_2,\mathbf{r}_3,\ldots,\mathbf{r}_{N_e}), \tag{24}$$

where $\rho_X^{eg}(\mathbf{r})$ is a one-electron transition-density for the excitation of the $X$ ($X=I$ or $J$) molecule. The interactions expressed in Eq. (23) were represented in a matrix as

$$V_{\mathrm{Coul}}^{\mathrm{TDFI}} = \sum_{\mu,\nu\in J} P_{\nu\mu}^J \sum_{\lambda,\sigma\in I} P_{\lambda\sigma}^I (\mu\nu|\sigma\lambda), \tag{25}$$

where $P_{\lambda\sigma}^X$ denotes the transition-density matrix between the ground and excited states for the $X$ ($X=I$ or $J$) molecule, and $(\mu\nu|\sigma\lambda)$ indicates a two-electron integral in an atomic orbital (AO) representation, i.e.,

$$(\mu\nu|\sigma\lambda) \equiv \int d\mathbf{r}_1 \int d\mathbf{r}_2 \phi_\mu^*(\mathbf{r}_1)\phi_\nu(\mathbf{r}_1) r_{12}^{-1} \phi_\sigma^*(\mathbf{r}_2)\phi_\lambda(\mathbf{r}_2), \tag{26}$$

where $\phi_i(\mathbf{r})$ is an AO. Equation (25) can be rewritten as

$$V_{\mathrm{Coul}}^{\mathrm{TDFI}} = \sum_{\mu,\nu\in J} P_{\nu\mu}^J V_{\mu\nu}^I, \tag{27}$$

where $V_{\mu\nu}^I$ denotes a "transition" potential generated by the molecule $I$. In the TDFI method, Eq. (27), is the expression for calculating the off-diagonal elements. It is noteworthy that TDFI is free from the aforementioned molecular center problem.

For computing the potential $V_{\mu\nu}^I$ in Eq. (27), the DFI algorithm[34] is used. First, the transition-density matrices $P_{\lambda\sigma}^a$ for the individual molecules, which have dimension $N_{\mathrm{AO}}^a \times N_{\mathrm{AO}}^a$ ($a=I$ or $J$), are calculated separately. Then, as shown in Fig. 1(a), the $N_{\mathrm{AO}}\times N_{\mathrm{AO}}$ total transition-density matrix $\mathbf{P}'_{\mathrm{tot}}$ is constructed by setting $P_{\lambda\sigma}^I$ and a zero matrix in corresponding diagonal blocks for the $I$ and $J$ molecules, respectively. The zero matrix for the $J$ block removes the self-Coulombic interaction within the $J$ molecule. Next, the $N_{\mathrm{AO}}\times N_{\mathrm{AO}}$ total transition potential matrix $\mathbf{V}_{\mathrm{int}}$ is constructed

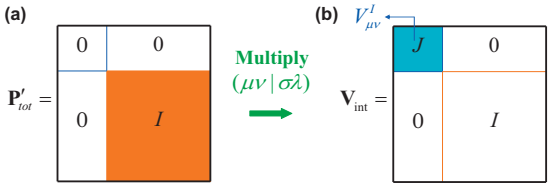


FIG. 1. Illustrations of (a) the total transition-density matrix and (b) the transition potential matrix.

by the product of $\mathbf{P}'_{\text{tot}}$ and the two-electron integrals, as shown in Fig. 1(b). Finally, the $N^J_{\text{AO}} \times N^J_{\text{AO}}$ portion, which is $V^I_{\mu\nu}$ in Eq. (27), is extracted from $\mathbf{V}_{\text{int}}$.

### D. Comparison with the transition-density cube method

A similar approach to compute the electronic coupling energy, called the transition-density cube (TDC) method, has been proposed by Krueger *et al.*[35] In the original paper, the TDC method performs spatial integrations in Eq. (23) numerically with the rectangle (cube in three-dimension spatial space) rule. The TDFI method has advantages over the TDC one in the following respects. First, the TDFI method carries out the spatial integrations in Eq. (23) with the AO two-electron integrals evaluated based on sophisticated quadratures conventionally used in quantum chemistry calculations, which are known to be more accurate than the rectangle rule used in the TDC method. Second, the TDFI method uses the self-consistent transition densities of the $I$ and $J$ molecules obtained with the DFI scheme,[34] whereas the TDC method computes the electronic coupling between the $I$ and $J$ densities that are separately calculated in gas-phase. In the DFI scheme, as described in Ref. 34, the DFI-Fock matrices of the $I$ and $J$ molecules in the $I/J$ complex include the external potentials from the counterpart $J$ and $I$ molecules, respectively, calculated with the electron density interactions between the $I$ and $J$ molecules, and the SCF procedure is iteratively continued until the total energy of the $I/J$ complex and the $I$ and $J$ electron densities are converged. Hence, the obtained transition densities also satisfy a self-consistency condition between the $I$ and $J$ molecules in the complex. Finally, the integral in Eq. (23) in the TDFI method is exactly equivalent to the corresponding integral in the DFI scheme for the density evaluations. The TDFI method therefore guarantees a strict consistency between the electronic coupling and the electron densities used.

Recently, the TDC method is gradually replaced by a direct evaluation of the Coulombic integral using the AO basis, which overcomes the integral problem associated with the original TDC method.[36–38] However, there still remains the problem on the self-consistency condition because transition densities obtained by single-fragment (molecule) excited state calculations are used.

The disadvantages of the TDC method are also overcome by the coupled frozen-density embedding (FDEc) method developed by Neugebauer,[39–42] which is a subsystem approach to time-dependent density functional theory (TD-DFT).[43] In addition, FDEc also covers non-Coulombic effects like exchange-correlation and orbital overlap effects[44] of the molecules $I$ and $J$, which are ignored in the present TDFI method because of the product *ansatz* in Eq. (7) and the explicit assumption of the orthogonal monomer wave functions.

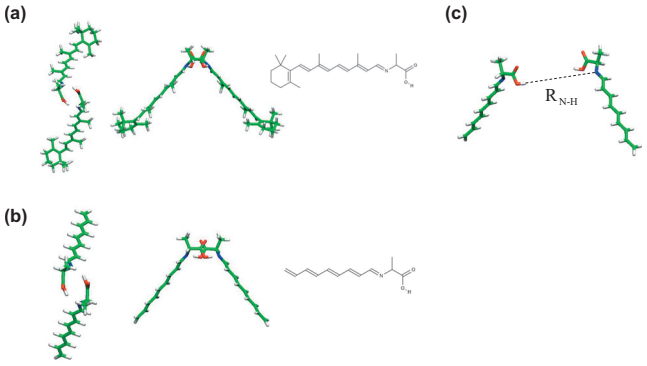


FIG. 2. Optimized structures of the $C_2$-symmetric (a) SB6 and (b) SB5 dimers. Left: top of view. Center: side view. Right: structural formula of monomer. In (c), the definition of the $x$-axis coordinate for Fig. 4 is shown.

## III. COMPUTATIONAL DETAILS

The all-*trans N*-retinylidene-L-alanine Schiff base (SB6) is known to exhibit the ECCD spectrum when it forms dimer.[29] In this study, the dimerized SB6 was selected as a computational model. To reduce computational costs, a model chromophore with five $\pi$-bonds (SB5) was also adopted. Using the dimerized SB5, the full quantum-mechanical (QM) calculations were performed for testing the TDFI accuracy.

The atomic coordinates were obtained via geometry optimization with density-functional theory (DFT) (Ref. 45) using the revised Coulomb-attenuating method (rCAM) B3LYP functional[46] and imposing $C_2$ symmetry. During optimization, the solvent effect of methylene chloride ($\varepsilon$=8.93) was included with the polarizable continuum model (PCM).[47] The optimized structures of SB6 and SB5 are shown in Figs. 2(a) and 2(b), respectively.

In the excited state calculations, TD-DFT (Ref. 43) with the B3LYP (Ref. 48) and rCAM-B3LYP functionals, and the symmetry-adapted cluster-CI (SAC-CI) (Ref. 49) method were employed for obtaining the excitation energies, the electric, magnetic, and velocity transition dipole moments, and the transition densities. In the SAC-CI calculations, double excitation operators were selected using a perturbation selection method.[50] All of single excitation operators and selected double excitation operators were included in the SAC and SAC-CI wave functions. In the perturbation selection of the double excitations, the level three threshold set, defined as $\lambda_g = 1.0 \times 10^{-6}$ hartree and $\lambda_e = 1.0 \times 10^{-7}$ hartree, was adopted. The $\lambda_g$ and $\lambda_e$ were energy thresholds used for the ground and excited states, respectively. In the TD-DFT calculations, the solvent effect of methylene chloride was included with PCM,[47] in which dielectric constant and dielectric constant at infinite frequency were set to the default values ($\varepsilon$=8.93 and $\varepsilon_\infty$=2.02).[51] To evaluate the solvent effects on the excitation-energy and the

TABLE I. Electronic coupling energies of the dimerized SB5 ($cm^{-1}$) (data in parentheses were calculated with TZVP basis set).

| | SAC-CI | TD-rCAM-B3LYP | TD-B3LYP |
|---|---|---|---|
| Full QM | 633.4 | 696.8 (685.9) | 741.1 (727.8) |
| TDFI | 612.9 | 667.3 (673.6) | 702.8 (708.2) |
| TrESP | 577.3 | 623.5 (629.9) | 646.4 (653.8) |
| dd | 1225.6 | 1346.0 (1389.9) | 1331.6 (1379.4) |

electronic coupling energy, the gas-phase calculations were also carried out with the same atomic coordinates as used in the PCM calculations.

In all calculations, the split valence double-$\zeta$ plus polarization basis set (6-31G*) was used for all atoms. In the excited state calculations, a frozen core approximation was applied to 1s core orbitals. The TDFI program with TD-DFT and SAC-CI was implemented in GAUSSIAN03.[52]

For calculating the CD curve, a Gaussian distribution was assumed for each transition, and the distributions were convoluted as follows:[10]

$$\Delta\varepsilon(E) = \frac{1}{2.296\times 10^{-39}\sqrt{\pi}\Delta\sigma}\sum_k E_{0k}R_{0k} \times\exp\left[-\left(\frac{E-E_{0k}}{\Delta\sigma}\right)^2\right], \quad (28)$$

where $E_{0k}$ and $R_{0k}$ are the excitation-energy and rotational strength from ground to the $k$th excited states for the exciton-coupled system, respectively, and $\Delta\sigma$ is the standard deviation of the Gaussian distribution. The value of $\Delta\sigma$ was taken to be 0.3 eV. In all cases, rotational strength was described in the velocity form and in cgs units (1 esu cm erg $G^{-1}$ $\approx 3.336\times 10^{-15}$ C m J $T^{-1}$ in SI units).

## IV. RESULTS

### A. Accuracy of the TDFI method

As a starting point for testing the TDFI accuracy, a dimerized SB5 compound shown in Fig. 2(b) was used as a computational model. In the matrix method, the off-diagonal element in the Hamiltonian matrix stands for the degree of exciton coupling (i.e., the electronic coupling). On the other hand, this value can be directly evaluated via a full-QM calculation of the dimerized molecule,

$$\langle\Phi_1|\hat{H}|\Phi_2\rangle = \tfrac{1}{2}(E'_a - E'_b), \quad (29)$$

where $E'_i$ denotes the $i$th excited state energy for the dimer. Equation (29) strictly holds only for symmetric dimers with identical monomer energies.[53] To estimate the error associated with the TDFI method, the value of Eq. (29) was taken as a reference, and the TDFI value was compared with it. In both of the full-QM and TDFI calculations, the SAC-CI, TD-rCAM-B3LYP, and TD-B3LYP methods were employed to understand the dependence on the electronic-structure method, as reported in previous studies.[54,55] As summarized in Table I, TDFI with SAC-CI, TD-rCAM-B3LYP, and TD-B3LYP provided 613, 667, and 703 $cm^{-1}$, respectively. Although the absolute value of the electronic coupling energy depends on the electronic-structure method used in the TDFI calculation ($\sim$90 $cm^{-1}$), all of computations with TDFI successfully reproduced the individual reference values (633, 697, and 741 $cm^{-1}$) with the deviations of 20–38 $cm^{-1}$. Therefore, we found that TDFI gives a quantitative value of the electronic coupling energy without regard to the electronic-structure method used. To check the basis set dependence, the TDFI and full-QM calculations at the TD-DFT (rCAM-B3LYP and B3LYP)/TZVP level were also performed. As listed in Table I, the TDFI values calculated with TD-rCAM-B3LYP and TD-B3LYP were to be 674 and 708 $cm^{-1}$, respectively, while the full-QM ones were to be 686 and 728 $cm^{-1}$, respectively. From these results, a small dependence of the coupling energy on the basis set was confirmed in the present system (TDFI: $\sim$7 $cm^{-1}$ and full-QM: $\sim$13 $cm^{-1}$).

As mentioned in Sec. II, the orthogonality between the electronic states of different molecules ($I$ and $J$) is assumed in the present TDFI scheme. To check this assumption, the overlap between two transition densities was evaluated by

$$\langle\Phi_1|\Phi_2\rangle = \sum_{\mu,\nu\in J}\sum_{\lambda,\sigma\in I} P^J_{\nu\mu}S_{\mu\lambda}P^I_{\lambda\sigma}S_{\sigma\nu}, \quad (30)$$

$$S_{\mu\lambda} \equiv \int d\mathbf{r}\,\phi^*_\mu(\mathbf{r})\phi_\lambda(\mathbf{r}), \quad (31)$$

where $P^X_{\nu\mu}$ denotes the transition-density matrix between the ground and excited states, and $S_{\mu\lambda}$ is the overlap matrix in the AO representation. As a result of calculations, negligibly small overlaps ($4.42\times 10^{-5}$, $5.05\times 10^{-5}$, and $6.75\times 10^{-5}$ from SAC-CI, TD-rCAM-B3LYP, and TD-B3LYP, respectively) were obtained, which indicates that an electron-exchange effect[56] originating from the antisymmetrization between two monomer electronic states is quite small. Thus, the validity of the assumption is confirmed in the present system.

To obtain further insight into the TDFI accuracy, the electronic coupling energy was calculated with other methods, and the results are also summarized in Table I. As found from this table, the dd method provided the electronic coupling of 1226–1346 $cm^{-1}$, which largely overestimated by 593–649 $cm^{-1}$ from the reference values. To clarify the difference between the TDFI and dd methods, the transition densities of SB5 were compared with their electric transition dipole moments. As shown in Fig. 3(a), the transition densities spread over each molecule. Because the electric transition dipole is represented as a point vector located at the molecular center defined by the center of mass of each molecule, such expanded transition-density cannot be described

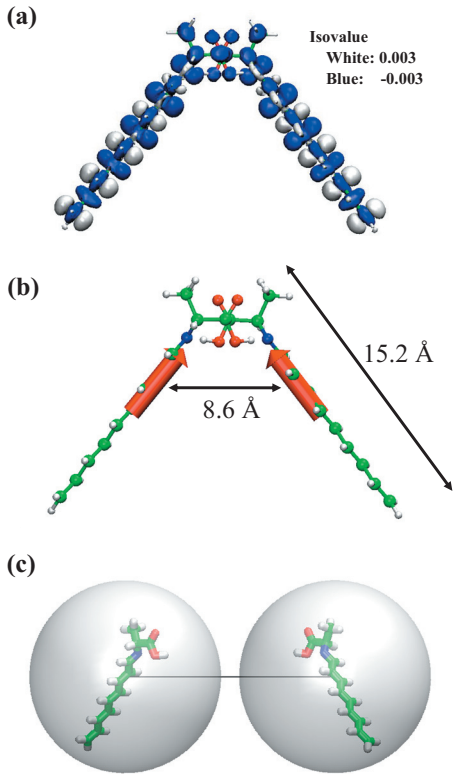


FIG. 3. (a) Transition-density distributions, (b) electric transition dipole moments, and (c) spheres enclosing the transition densities. In (b), red arrows show the electric transition dipole moments located at the center of mass of the individual SB5 chromophores. In (c), the radius is taken to be 9.5 Å and the intermolecular N–H distance and the center-to-center distance are 17.0 and 20.9 Å, respectively.

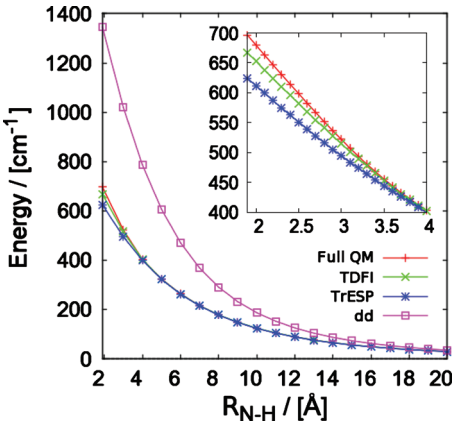


FIG. 4. Electronic coupling energies between two SB5 chromophores as a function of intermolecular N–H distance. (+) Full quantum-mechanical, (×) TDFI, ( *) TrESP, and (□) dd results. All calculations are performed with TD-rCAM-B3LYP/6-31G*.

accurately by the electric transition dipole. As shown in Fig. 3(b), the center-to-center separation between two SB5 chromophores (8.6 Å) is smaller than the individual molecular sizes (~15.2 Å). Thus, a slight difference in definition of the molecular center gives rise to a large change of the electronic coupling. This is a reason why the dd results are quite different from the TDFI ones.

In our previous study, the transition charge from ESP (TrESP) method[57] was also used for computing the electronic coupling energy between salinixanthin and retinal chromophores, which resulted in almost the same value as the TDFI one with the deviation of 2 $cm^{-1}$ (see Appendix for details).[26] However, the present results with TrESP are to be 577–646 $cm^{-1}$, which are different by 36–57 and 56–95 $cm^{-1}$ from the TDFI and reference values, respectively. To clearly show the difference between TDFI and TrESP, the electronic coupling energies were calculated along with the separation between two SB5 chromophores. The definition of the $x$-axis coordinate is illustrated in Fig. 2(c). As shown in Fig. 4, while the TrESP method gives similar values to TDFI in the large separation, the difference gradually becomes larger with the decrease in the molecular separation. At less than 2.5 Å, the energy difference between TrESP and TDFI becomes more than 30 $cm^{-1}$. This is because the TrESP method uses the gas-phase transition charges. In other words, TrESP does not satisfy a self-consistency condition between the transition densities of two chromophores, which leads to the deviation from the TDFI value. This result indicates a significant role of the self-consistent treatment for the accurate description of the electronic coupling. Similarly, the dd calculations were carried out along with the molecular separation and the results are also shown in Fig. 4. Differently from the TDFI and TrESP results, the dd method overestimated the electronic coupling energies in all the regions. The deviation from the reference value becomes smaller with the increase in the molecular separation and then the 10 $cm^{-1}$ accuracy is satisfied at 17 Å. As illustrated in Fig. 3(c), two spheres that enclose the individual molecules (transition densities) have no overlap at 17 Å, which indicates that the multipole expansion of the electronic coupling is valid in this region. From these results, it was confirmed that the TDFI description for the electronic coupling is more accurate than the conventional dd and TrESP methods.

### B. The ECCD spectrum of the dimerized SB6

Based on the successful description of the electronic coupling (i.e., the off-diagonal element), the matrix method combined with TDFI was applied to the full-length chromophore (SB6) [Fig. 2(a)], and the ECCD spectrum observed in methylene chloride solution was investigated. It is noted that since the full quantum-mechanical calculation for this system could not be performed due to computational restrictions, the experimental spectral data[29] were used as a reference instead of Eq. (29). The first excited state, which is characterized as a $\pi$-$\pi^*$ excitation from the highest occupied molecular orbital to the lowest unoccupied molecular orbital,[58,59] is discussed here.

Table II summarizes the excitation-energy and rotational strength calculated with SAC-CI, TD-B3LYP, and TD-rCAM-B3LYP. Here, it is noted that while the TD-B3LYP and TD-rCAM-B3LYP calculations were performed with PCM for describing the solvent effect, the SAC-CI calculation was done only with the reaction field obtained from the Hartree–Fock ground state since the present SAC-CI code is not connected to the self-consistent reaction field PCM one. On the excitation-energy, SAC-CI and TD-B3LYP provided 3.50 and 3.15 eV, respectively,

TABLE II. Excitation energies, electronic coupling energies, and rotational strength of SB6. (data in parentheses were calculated in the gas-phase. The atomic coordinate used was the same as that in methylene chloride.)

| | TD-B3LYP | TD-rCAM-B3LYP | SAC-CI | Expt.[a] |
|---|---|---|---|---|
| $E_{ex}$ (eV) | 3.15 (3.31) | 4.00 (4.17) | 3.50 (3.52) | 3.26 |
| $V_{Coul}$ ($cm^{-1}$) | 252.8 (447.6) | 327.8 (612.5) | 517.8 (510.6) | ⋯ |
| $R$ ($10^{-40}$ cgs) | −15.0 (−25.5) | 44.0 (36.9) | −12.8 (−13.4) | ⋯ |

[a]Reference 29.

which could well reproduce the experimental value (3.26 eV) with the deviations of 0.24 and 0.11 eV, respectively. On the other hand, the TD-rCAM-B3LYP calculation (4.00 eV) resulted in the large overestimation of 0.74 eV. To clarify the solvent effect, the gas-phase calculations were also carried out with the same geometry used in the methylene chloride calculations. As also summarized in Table II, the calculated excitation energies with SAC-CI, TD-B3LYP, and TD-rCAM-B3LYP were to be 3.52, 3.31, and 4.17 eV, respectively. From the comparison with the methylene chloride results, we found the solvent effect brought about the spectral redshifts of 0.02, 0.16, and 0.17 eV for SAC-CI, TD-B3LYP, and TD-rCAM-B3LYP, respectively. Here, the SAC-CI result shows the smaller solvent effect, which is due to the lack of the PCM treatment.

Regarding the electronic coupling, the TDFI calculations with SAC-CI, TD-B3LYP, and TD-rCAM-B3LYP provided 518, 253, and 328 $cm^{-1}$, respectively, as also listed in Table II. In spite of the agreement of the SAC-CI excitation-energy with the experimental value, the electronic coupling energy obtained with SAC-CI gave rise to large differences by 265 and 190 $cm^{-1}$ from those with TD-B3LYP and TD-rCAM-B3LYP, respectively. This was also caused by the lack of the PCM treatment in the SAC-CI calculation. Similarly to the excitation-energy, the gas-phase calculations of the electronic coupling were performed, which are also summarized in Table II. As found from this table, the solvent effect reduced the electronic coupling energies obtained with TD-B3LYP (448 $cm^{-1}$) and TD-rCAM-B3LYP (613 $cm^{-1}$) by 195 and 285 $cm^{-1}$, respectively. From these results, a large contribution of the solvent effect to the electronic coupling was confirmed, as reported in previous studies.[44,60–62] By also considering the excitation-energy results, the TD-B3LYP values were used for the CD spectral calculation.

As mentioned above, the matrix method commonly approximates the diagonal elements to the excitation energies of the noninteracting molecules. To check the validity of this approximation, the rest contributions were estimated. Equations (19) and (20) can be rewritten in matrix form as

$$\langle\Phi_1|\hat{H}|\Phi_1\rangle = E_{ex}^I + \sum_{\mu,\nu\in I}(P_{\nu\mu}^{Ie} - P_{\nu\mu}^{Ig}) \times\left[V_{\mu\nu}^{nuclJ} + \sum_{\lambda,\sigma\in J} P_{\lambda\sigma}^{Jg}(\mu\nu|\sigma\lambda)\right], \quad (32)$$

$$\langle\Phi_2|\hat{H}|\Phi_2\rangle = E_{ex}^J + \sum_{\mu,\nu\in J}(P_{\nu\mu}^{Je} - P_{\nu\mu}^{Jg}) \times\left[V_{\mu\nu}^{nuclI} + \sum_{\lambda,\sigma\in I} P_{\lambda\sigma}^{Ig}(\mu\nu|\sigma\lambda)\right], \quad (33)$$

$$V_{\mu\nu}^{nuclX} \equiv \int d\mathbf{r}_1 \phi_\mu^*(\mathbf{r}_1)\left[\sum_{A\in X}^{nucl}\frac{-Z_A}{r_{1A}}\right]\phi_\nu(\mathbf{r}_1), \quad (34)$$

where $P_{\nu\mu}^{Xs}$ denotes the one-electron density matrix of the $X$ molecule in the state $s$ ($s$=ground or excited states) and $V_{\mu\nu}^{nuclX}$ expresses the nuclear potential generated by the molecule $X$. Since Eqs. (32) and (33) correspond to the excitation energies that include the electronic polarization effects induced by the Coulombic interactions with the counterpart molecule, these values can be computed with the DFI method.[34] As a result of the DFI calculations, the excitation-energy of 3.10 eV was obtained, which indicated the spectral redshift of 0.05 eV compared with the excitation-energy of the monomer in methylene chloride (3.15 eV). Taking into account the spectral redshift caused by the solvent effect (0.16 eV), the contribution from the electronic polarization effect was smaller by 0.11 eV than that from the solvent effect. From these results, it was confirmed that since the electronic polarization effect is the minor contribution to the spectral shift, the conventional approximation reasonably represents the diagonal elements.

Using the calculated values (i.e., the excitation energies and the electronic coupling energies), the Hamiltonian matrix was constructed and then it was diagonalized. As a result, the excitation energies obtained from the eigenvalues were to be 3.07 eV (404 nm) and 3.13 eV (396 nm). From the comparison with the excitation-energy of the non-exciton-coupled system (3.10 eV), the spectral shifts due to the exciton coupling were estimated to be −0.03 and 0.03 eV for the lower and higher excited states, respectively. Using Eqs. (5), (12), and (13), the rotational strength of the exciton-coupled system was computed, which resulted in $-3898\times10^{-40}$ and $3790\times10^{-40}$ cgs at 3.07 and 3.13 eV, respectively. Because the rotational strength of the non-exciton-coupled system was $-15\times10^{-40}$ cgs, a significant enhancement of the rotational strength by the exciton coupling was found.

Next, the CD spectral curve was calculated using Eq. (28). As illustrated in Fig. 5, the obtained CD spectrum becomes a bisignate curve in which negative and positive peaks (Cotton effects) appear at 429 nm (2.89 eV) and 373 nm (3.32 eV), respectively. Therefore, this result is interpreted as a negative chirality, and such a character can also be expected with the exciton chirality method because the chirality of the electric transition dipole moments is anticlockwise.[10] Figure 5 also shows the two component CD curves in which the negative and positive peak positions at 404 nm (3.07 eV) and 396 nm (3.13 eV), respectively, are separated by a Davydov splitting[63,64] of $2V_{Coul}^{TDFI}$=506 $cm^{-1}$. Convolution of two component CD curves gave rise to the

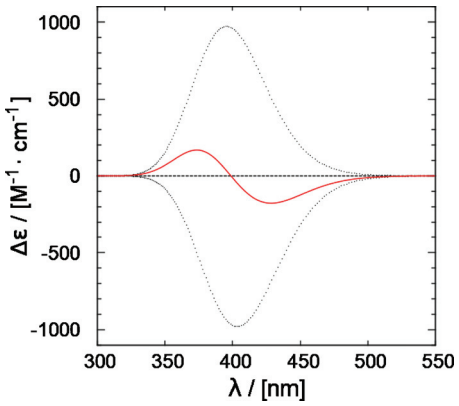


FIG. 5. Theoretical CD spectrum of the dimerized SB6. The solid line is the total CD curve and the dotted lines are the component CD ones.

apparent splitting of 3472 $cm^{-1}$, which was in excellent agreement with the experimental value (3217 $cm^{-1}$: first and second Cotton effects at 420 and 370 nm, respectively).[29]

## V. CONCLUSIONS

In this paper, the TDFI approach for the ECCD spectra was proposed. TDFI is based on the electronic Coulombic interactions between the transition densities for the individual molecules, which can be applied to the matrix method for calculating the ECCD spectra. Compared with the conventional dd and TrESP methods, TDFI has a much improved description of the electronic coupling. In addition, the TDFI scheme can be easily extended to other electronic-structure methods and is free from the center problem associated with the dd method. These advantages make it possible to quantitatively reproduce the experimental ECCD spectra. Hence, the matrix method combined with TDFI can reduce the computational costs compared with the full quantum-mechanical calculations, so that it is expected to be useful for large molecules. As a result of the application to the dimerized SB6, the present approach succeeded in accurately estimating the two CD Cotton effects observed in experiment, whereas such a large calculation could not be performed with the full quantum-mechanical method.

In this study, the treatment of the diagonal element in the Hamiltonian matrix was also discussed. In common cases, the matrix method approximates the diagonal elements to the excitation-energy for the noninteracting molecules because the contributions from the external field are considered as negligible. However, there was not enough evidence to confirm this assumption. The DFI method allowed us to compute the more accurate value of the diagonal element and the electronic polarization effect induced by the intermolecular interactions could be estimated. As a result, the contribution of the electronic polarization effect was found to be small, so that the quantitative evaluation could support the conventional assumption to be reasonable.

The present CD spectral calculation was performed on the basis of the TD-B3LYP results. Although the SAC-CI calculation well reproduced the experimental excitation-energy, it largely overestimated the electronic coupling energy due to the lack of the PCM treatment. It is, therefore, desirable to have PCM implemented into the SAC-CI code. Because most of the experimental CD measurements are performed in solvent system, such a higher order theory with PCM would enable one to study various chiral compounds and provide new insights into the observed CD spectra.

## ACKNOWLEDGMENTS

This study was supported by a Grant-in-Aid for Young Scientists (B) from the Japan Society for the Promotion of Science (JSPS) and the Global COE program from the Ministry of Education, Culture, Sports, Sciences, and Technology of Japan.

## APPENDIX: THE TRESP METHOD

In the TrESP method,[57] the electronic coupling energy is represented by classical Coulombic interaction between the "transition" charges which are determined with transition-density by a scheme analogous to the electrostatic potential (ESP) fitted charge method[65] widely used for classical description of ESP. To obtain the fitted transition charges, the following function is used for a least square fitting:

$$Z = \sum_i^m \left( V_i - \sum_j^n \frac{q_j}{r_{ij}} \right)^2 + \lambda \left( \sum_j^n q_j - q_{\mathrm{tot}} \right), \tag{A1}$$

where $\lambda$ denotes Lagrange multiplier for the constraint of the charges. For the determination of the transition changes, the total charge in the constraint is set to be zero because of the orthogonality between the ground and excited states,

$$q_{\mathrm{tot}} = 0. \tag{A2}$$

Equation (A2) is also applied to ionic molecules. The nuclear contributions are also excluded from the transition potential, $V_i$, in Eq. (A1) also due to the orthogonality. In other words, only the electronic contributions are necessary for Eq. (A1). The transition potential at point $i$ is represented as follows:

$$V_i = -\sum_{\mu,\nu \in X} P^X_{\nu\mu} \int d\mathbf{r}_1 \phi^{X^*}_\mu(\mathbf{r}_1) r^{-1}_{1i} \phi^X_\nu(\mathbf{r}_1), \tag{A3}$$

where $P^X_{\nu\mu}$ denotes the transition-density matrix between the ground and excited states, and $\int d\mathbf{r}_1 \phi^{X^*}_\mu(\mathbf{r}_1) r^{-1}_{1i} \phi^X_\nu(\mathbf{r}_1)$ is the one-electron integral in an AO representation. The rest of the procedure is the same as the case of the ESP fitted charges. The transition charges are then determined by solving a linear equation,

$$\begin{pmatrix} A_{11} & A_{12} & \cdots & A_{1n} & 1 \\ A_{21} & A_{22} & \cdots & A_{2n} & 1 \\ \vdots & \vdots & \ddots & \vdots & 1 \\ A_{n1} & A_{n2} & \dots & A_{nn} & 1 \\ 1 & 1 & 1 & 1 & 0 \end{pmatrix} \begin{pmatrix} q_1 \\ q_2 \\ \vdots \\ q_n \\ \lambda \end{pmatrix} = \begin{pmatrix} B_1 \\ B_2 \\ \vdots \\ B_n \\ 0 \end{pmatrix}, \tag{A4}$$

where

$$A_{jk} = \sum_i^m \frac{1}{r_{ij} r_{ik}}, \tag{A5}$$

$$B_k = \sum_i^m \frac{V_i}{r_{ik}}. \quad \text{(A6)}$$

Finally, the electronic coupling energy is calculated with the obtained charges,

$$V_{\text{Coul}}^{\text{TrESP}} = \sum_{i\in I}\sum_{j\in J}\frac{q_i q_j}{r_{ij}}. \quad \text{(A7)}$$


[1] *Circular Dichroism: Principles and Applications*, edited by N. Berova, K. Nakanishi, and R. W. Woody (Wiley-VCH, New York, 2000).
[2] S. Beychok, Science **154**, 1288 (1966).
[3] N. J. Greenfield and G. D. Fasman, Biochemistry **8**, 4108 (1969).
[4] N. J. Greenfield, Nat. Protoc. **1**, 2876 (2007).
[5] L. Whitmore and B. A. Wallace, Biopolymers **89**, 392 (2007).
[6] J. W. Lewis, R. F. Tilton, C. M. Einterz, S. J. Milder, I. D. Kuntz, and D. S. Kliger, J. Phys. Chem. **89**, 289 (1985).
[7] C.-F. Zhang, J. W. Lewis, R. Cerpa, I. D. Kuntz, and D. S. Kliger, J. Phys. Chem. **97**, 5499 (1993).
[8] S. C. Björling, C.-F. Zhang, D. S. Kliger, D. L. Farrens, and P.-S. Song, J. Am. Chem. Soc. **114**, 4581 (1992).
[9] E. Chen, P. Wittung-Stafshede, and D. S. Kliger, J. Am. Chem. Soc. **121**, 3811 (1999).
[10] N. Harada and K. Nakanishi, *Circular Dichroic Spectroscopy: Exciton Coupling in Organic Stereochemistry* (University Science Books, Mill Valley, CA, 1983).
[11] W. Kuhn, Trans. Faraday Soc. **26**, 293 (1930).
[12] J. G. Kirkwood, J. Chem. Phys. **5**, 479 (1937).
[13] I. Tinoco, Jr., J. Am. Chem. Soc. **82**, 4785 (1960).
[14] R. W. Woody and I. Tinoco, Jr., J. Chem. Phys. **46**, 4927 (1967).
[15] R. W. Woody, J. Chem. Phys. **49**, 4797 (1968).
[16] J. A. Schellman, Acc. Chem. Res. **1**, 144 (1968).
[17] W. C. Johnson, Jr., and I. Tinoco, Jr., Biopolymers **8**, 715 (1969).
[18] I. Tinoco, Jr., Adv. Chem. Phys. **4**, 113 (1962).
[19] P. M. Bayley, E. B. Nielsen, and J. A. Schellman, J. Phys. Chem. **73**, 228 (1969).
[20] J. Frenkel, Phys. Rev. **37**, 1276 (1931).
[21] W. J. Goux and T. M. Hooker, Jr., J. Am. Chem. Soc. **102**, 7080 (1980).
[22] J. D. Hirst, J. Chem. Phys. **109**, 782 (1998).
[23] N. A. Besley and J. D. Hirst, J. Am. Chem. Soc. **121**, 9636 (1999).
[24] N. Sreerama and R. W. Woody, Methods Enzymol. **383**, 318 (2004).
[25] N. Harada and K. Nakanishi, J. Am. Chem. Soc. **91**, 3989 (1969).
[26] K. J. Fujimoto and S. Hayashi, J. Am. Chem. Soc. **131**, 14152 (2009).
[27] T. Förster, Ann. Phys. **437**, 55 (1948).
[28] T. Förster, in *Modern Quantum Chemistry*, edited by O. Sinanoglu (Academic, New York, 1965), Vol. III, p. 93.
[29] Y. Gat and M. Sheves, Photochem. Photobiol. **59**, 371 (1994).
[30] L. Rosenfeld, Z. Phys. **52**, 161 (1928).
[31] A. J. McHugh and M. Gouterman, Theor. Chim. Acta **13**, 249 (1969).
[32] A. Warshel and W. W. Parson, J. Am. Chem. Soc. **109**, 6143 (1987).
[33] W. Moffitt, J. Chem. Phys. **25**, 467 (1956).
[34] K. Fujimoto and W.-T. Yang, J. Chem. Phys. **129**, 054102 (2008).
[35] B. P. Krueger, G. D. Scholes, and G. R. Fleming, J. Phys. Chem. B **102**, 5378 (1998).
[36] C. Curutchet and B. Mennucci, J. Am. Chem. Soc. **127**, 16733 (2005).
[37] V. Russo, C. Curutchet, and B. Mennucci, J. Phys. Chem. B **111**, 853 (2007).
[38] C.-P. Hsu, Z.-Q. You, and H.-C. Chen, J. Phys. Chem. C **112**, 1204 (2008).
[39] J. Neugebauer, J. Chem. Phys. **126**, 134116 (2007).
[40] J. Neugebauer, J. Phys. Chem. B **112**, 2207 (2008).
[41] J. Neugebauer, J. Chem. Phys. **131**, 084104 (2009).
[42] J. Neugebauer, ChemPhysChem **10**, 3148 (2009).
[43] R. Bauernschmitt and R. Ahlrichs, Chem. Phys. Lett. **256**, 454 (1996).
[44] C.-P. Hsu, G. R. Fleming, M. Head-Gordon, and T. Head-Gordon, J. Chem. Phys. **114**, 3065 (2001).
[45] W. Kohn and L. J. Sham, Phys. Rev. **140**, A1133 (1965).
[46] A. J. Cohen, P. Mori-Sánchez, and W.-T. Yang, J. Chem. Phys. **126**, 191109 (2007).
[47] M. T. Cancès, B. Mennucci, and J. Tomasi, J. Chem. Phys. **107**, 3032 (1997).
[48] C. Lee, W.-T. Yang, and R. G. Parr, Phys. Rev. B **37**, 785 (1988).
[49] H. Nakatsuji, Chem. Phys. Lett. **59**, 362 (1978).
[50] H. Nakatsuji, Chem. Phys. **75**, 425 (1983).
[51] M. Cossi and V. Barone, J. Phys. Chem. A **104**, 10614 (2000).
[52] M. J. Frisch, G. W. Trucks, H. B. Schlegel *et al.*, GAUSSIAN03, Gaussian Inc., Pittsburgh, PA, 2003.
[53] S. Tretiak, C. Middleton, V. Chernyak, and S. Mukamel, J. Phys. Chem. B **104**, 4519 (2000).
[54] A. Muñoz-Losa, C. Curutchet, I. F. Galván, and B. Mennucci, J. Chem. Phys. **129**, 034104 (2008).
[55] E. Sagvolden, F. Furche, and A. Köhn, J. Chem. Theory Comput. **5**, 873 (2009).
[56] D. L. Dexter, J. Chem. Phys. **21**, 836 (1953).
[57] M. E. Madjet, A. Abdurahman, and T. Renger, J. Phys. Chem. B **110**, 17268 (2006).
[58] K. Fujimoto, S. Hayashi, J. Hasegawa, and H. Nakatsuji, J. Chem. Theory Comput. **3**, 605 (2007).
[59] K. Fujimoto, J. Hasegawa, and H. Nakatsuji, Bull. Chem. Soc. Jpn. **82**, 1140 (2009).
[60] M. F. Iozzi, B. Mennucci, J. Tomasi, and R. Cammi, J. Chem. Phys. **120**, 7029 (2004).
[61] C. Curutchet, G. D. Scholes, B. Mennucci, and R. Cammi, J. Phys. Chem. B **111**, 13253 (2007).
[62] J. Neugebauer, C. Curutchet, A. Muñoz-Losa, and B. Mennucci, J. Chem. Theory Comput. **6**, 1843 (2010).
[63] A. S. Davydov, Zh. Eksp. Teor. Fiz. **18**, 210 (1948).
[64] A. S. Davydov, *Theory of Molecular Excitons* (McGraw-Hill, New York, 1962).
[65] U. C. Singh and P. A. Kollman, J. Comput. Chem. **5**, 129 (1984).